ELSEVIER

Combined quantum mechanical and molecular mechanical reaction pathway calculation for aromatic hydroxylation by p-hydroxybenzoate-3-hydroxylase

Lars Ridder,* Adrian J. Mulholland,† Ivonne M.C.M. Rietjens,* and Jacques Vervoort*

**Laboratory of Biochemistry, Wageningen University, Wageningen, The Netherlands*
†School of Chemistry, University of Bristol, Bristol UK

The reaction pathway for the aromatic 3-hydroxylation of p-*hydroxybenzoate by the reactive C4a-hydroperoxyflavin cofactor intermediate in* p-*hydroxybenzoate hydroxylase (PHBH) has been investigated by a combined quantum mechanical and molecular mechanical (QM/MM) method. A structural model for the C4a-hydroperoxyflavin intermediate in the PHBH reaction cycle was built on the basis of the crystal structure coordinates of the enzyme–substrate complex. A reaction pathway for the subsequent hydroxylation step was calculated by imposing a reaction coordinate that involves cleavage of the peroxide oxygen–oxygen bond and formation of the carbon–oxygen bond between the C_3 atom of the substrate and the distal oxygen of the peroxide moiety of the cofactor. The geometric changes and the Mulliken charge distributions along the calculated reaction pathway are in line with an electrophilic aromatic substitution type of mechanism. The energy barrier of the calculated reaction is considerably lower when the substrate hydroxyl moiety is deprotonated, in comparison with the barrier found with a protonated hydroxyl moiety. This effect of the protonation state of the substrate on the calculated energy barrier supports experimental observations that deprotonation is required for hydroxylation of the substrate. A notable event in the calculated reaction pathway is a lengthening of the peroxide oxygen–oxygen bond at an intermediate stage. Further analysis of the reaction pathway indicates that this oxygen–oxygen bond elongation is accompanied by an increase in electrophilic reactivity on the distal oxygen of the peroxide moiety, which may assist the C–O bond formation in the reaction of the C4a-hydroperoxyflavin intermediate with the substrate. Analysis of the effect of individual active site residues on the reaction reveals a specific transition state stabilization by the backbone carbonyl moiety of Pro293. The crystal water 717 appears to drive the hydroxylation step through a stabilizing hydrogen bond interaction to the proximal oxygen of the C4a-hydroperoxyflavin intermediate, which increases in strength as the hydroperoxyflavin cofactor converts to the anionic (deprotonated) hydroxyflavin. © 2000 by Elsevier Science Inc.*

Keywords: QM/MM, PHBH, electrophilic aromatic substitution, substrate activation, cofactor activation

Color Plates for this article are on page 214.

Corresponding author: L. Ridder, Laboratory of Biochemistry, Wageningen University, Dreijenlaan 3, 6703 HA Wageningen, The Netherlands. Tel.: + 31-317-482868; fax: + 31-317-484801.

E-mail address: Lars.Ridder@p450.bc.wau.nl (L. Ridder)

INTRODUCTION

The flavoprotein monooxygenase *p*-hydroxybenzoate hydroxylase (PHBH, EC 1.14.13.2), catalyzes the 3-hydroxylation of *p*-hydroxybenzoate, which is an important step in the microbial degradation pathways of a wide variety of aromatic compounds. The first steps in the reaction cycle of PHBH involve binding of the substrate followed by a two-electron reduction of the flavin cofactor by NADPH and the incorporation of molecular oxygen to form the C4a-peroxyflavin intermediate. On protonation of the distal oxygen of the C4a-peroxyflavin, the so-called C4a-hydroperoxyflavin is formed, which reacts with the substrate and leads to the formation of the hydroxylated product and the hydroxyflavin form of the cofactor. Finally, release of water from the hydroxyflavin leads to the formation of the original oxidized state of the flavin cofactor. The attack of the C4a-hydroperoxyflavin on the substrate has previously been suggested to be rate limiting at pH 8, 25°C.[1]

Journal of Molecular Graphics and Modelling 17, 163–175, 1999

655 Avenue of the Americas, New York, NY 10010

1093-3263/99/$–see front matter
PII S1093-3263(99)00027-3

Two questions concerning the mechanism of hydroxylation have been the subject of several studies. First, the required protonation states of the substrate and of the activated cofactor for the hydroxylation reaction are of interest. Deprotonation of the hydroxyl moiety at C_4 of the aromatic substrate is suggested to be essential for its conversion. This conclusion was originally based on the observation that compounds lacking this hydroxyl moiety are not converted.[2] Furthermore, studies on the Tyr201Phe mutant enzyme indicate that a hydrogen bond network formed by Tyr201 and Tyr385 has a crucial role in deprotonating the substrate in the active site. The considerable decrease in efficiency of hydroxylation in the mutant, as a result of a loss of substrate deprotonation, further supports the proposal that the deprotonation of the substrate hydroxyl moiety in wild-type enzyme is needed to activate the substrate for hydroxylation.[3,4] Molecular orbital studies of the *p*-hydroxybenzoate substrate have demonstrated that deprotonation increases the nucleophilic reactivity of the C_3 centre in the substrate, which could be essential for an electrophilic attack on this C_3 centre by the C4a-(hydro)peroxyflavin cofactor.[1] With respect to the protonation state of the C4a-peroxyflavin cofactor, some information comes from transient kinetic studies of a related flavin-dependent aromatic hydroxylase, phenol hydroxylase from *Trichosporon cutaneum*.[5] In these experiments several intermediates were observed, two of which were ascribed to, respectively, the unprotonated and protonated form of the flavin intermediate, i.e., to the C4a-peroxyflavin and to the C4a-hydroperoxyflavin. This experimental observation supports the proposal that the peroxide moiety becomes protonated to activate the peroxyflavin for the transfer of oxygen to the substrate C_3.

A second major question with respect to the catalytic mechanism of PHBH concerns the splitting of the peroxide dioxygen bond in the hydroxylation step. Mechanisms involving heterolytic cleavage[6,7] as well as mechanisms involving homolytic cleavage[7–10] of the peroxide oxygen–oxygen bond have been proposed. At present, one of the earliest suggestions of electrophilic aromatic substitution involving heterolytic cleavage of the peroxide bond is supported by experimental data.[5] However, definite evidence with respect to the exact reaction mechanism seems to be lacking, which is mainly due to the short lifetime of the reaction intermediates that are formed on hydroxylation. This makes it difficult to obtain detailed experimental information on the nature of this hydroxylation step and the reaction intermediates formed.

In the present study, a combined quantum mechanical and molecular mechanical (QM/MM) reaction pathway analysis of the hydroxylation step in the PHBH reaction cycle has been performed. The combination of quantum mechanics and molecular mechanics is a promising approach to describe enzymatic reactions within the environment of the protein.[11–15] Quantum chemical (QM) treatment is preferred for chemical reactions, which involve breaking and forming of bonds and electronic redistribution. On the other hand, molecular mechanical (MM) methods are more practical for large protein structures. In QM/MM methods, a molecular system is separated into a small quantum mechanical region, describing the reacting part of the system (substrate, cofactor, and/or catalytic amino acids), and a molecular mechanical region describing the surrounding protein and solvent molecules.[16]

The validity of the present reaction pathway model for the hydroxylation in the PHBH reaction cycle, obtained with the QM/MM method described by Field et al.,[17] has been demonstrated previously through the correlation of the calculated energy barriers for the hydroxylation of a series of fluorinated substrate derivatives with experimental rate constants for the conversion of these substrates by PHBH.[18] In the present study this QM/MM reaction pathway model is applied to yield additional insight into the mechanism of the hydroxylation reaction catalyzed by PHBH and the electronic characteristics of the intermediates.

METHODS

Preparation of the protein model

A three-dimensional structure of the C4a-hydroperoxyflavin–substrate intermediate of PHBH was built on the basis of the crystal structure of oxidized PHBH in complex with the substrate *p*-hydroxybenzoate[19,20] obtained from the Protein Data-Bank (entry code 1PBE.PDB). Two other crystal structures, of the reduced PHBH–substrate complex and of the PHBH–product complex, are similar to the structure of the oxidized PHBH–substrate complex.[20,21] On the basis of this similarity, no dramatic changes in the protein conformation around the active site are expected for the C4a-hydroperoxyflavin intermediate in the reaction cycle and during the subsequent reaction step.

The flavin cofactor present in the crystal structure in its resting state was modified to the active C4a-hydroperoxyflavin intermediate using the coordinates reported by Schreuder et al.[22] on the basis of molecular modeling studies and experimental NMR data of the C4a-hydroperoxyflavin intermediate.[23] Hydrogen atoms were added to the protein according to an extended atom topology (i.e., only polar group hydrogens were modeled explicitly), using CHARMM.[24] An all-hydrogen topology was used for the substrate and the isoalloxazine ring of the cofactor, because this part of the structure was treated quantum mechanically. The hydroxyl and carboxyl moieties of the substrate were modeled in the anionic state. The coordinates of 330 water molecules in the crystal structure were used to build explicit water molecules in the model, using the HBUILD routine of the CHARMM program. Since in this structure the substrate and the peroxide moiety of the cofactor are not exposed to solvent it was not considered necessary to add more water molecules to the model.

QM/MM calculations

On the basis of the starting geometry described above, QM/MM calculations were performed using CHARMM version 24b1.[24] The C4a-hydroperoxyflavin and the dianionic substrate were treated quantum mechanically on the basis of a closed shell semiempirical AM1 Hamiltonian.[25] The covalent C–C bond between the C_1* and the C_2* of the ribityl chain of the FAD cofactor, which crosses the boundary between the QM and MM regions, was replaced by a C–QQH (link atom) bond in the QM system.[17] All other atoms were treated at the molecular mechanical level (MM), using the CHARMm 22 forcefield.[26] The complete simulation system consists of 50 QM atoms, and 4 840 MM atoms. The QM region has a total charge of $-2e$. All energies were evaluated with a nonbonded cutoff distance of 11 Å, using a group-based switching function to smooth the QM/MM interactions to zero. The coordinates of

295 atoms within a 10-Å sphere around the distal oxygen of the cofactor were optimized to a gradient tolerance of 0.01 kcal mol^{-1} $Å^{-1}$ (1 cal = 4.184 J), requiring 780 steps of adopted basis Newton–Raphson (ABNR) minimization. This geometry-optimized region included the substrate, the flavin ring, (parts of) 37 amino acid residues in the active site, and 15 water molecules. All other atoms were fixed during the calculations.

Validation of AM1 for the QM system

In the model described above the substrate and the flavin ring of the cofactor were treated quantum mechanically (QM) by the semiempirical AM1 method. This QM system has a total charge of $-2e$. In the case of *ab initio* methods, calculations on anions require basis sets with diffuse functions. Semiempirical methods, such as AM1, use minimal basis sets, which do not include diffuse functions. Nevertheless, AM1 often performs well on anionic systems and appears to be able to correct for the increased electron repulsion through the parameterization.[25] The competence of AM1 for even a dianionic system is illustrated by a recent comparison of AM1 with *ab initio* methods for dianionic oxaloacetate, for which the AM1 results were similar to those from *ab initio* calculations including diffuse functions and performed even better than *ab initio* methods without diffuse functions.[27]

To test AM1 for the dianionic QM system in the present PHBH model, gas-phase calculations were performed for the separate reactants, *p*-hydroxybenzoate and C4a-hydroperoxyflavin, and the expected products, hydroxycyclohexadienone and ionized hydroxyflavin, and the results were compared with *ab initio* calculations including diffuse functions. These gas-phase calculations were performed with Spartan version 5.1[28] and Gaussian 98,[29] using the AM1, HF/6-31+G(d), and B3LYP/6-31+G(d) methods.

Definition of the reaction pathway

The QM/MM model for the C4a-hydroperoxyflavin–substrate intermediate was used as a starting geometry for a reaction pathway calculation describing the reaction of the C4a-hydroperoxyflavin with the substrate. Figure 1 schematically presents this hydroxylation reaction according to an electrophilic aromatic substitution mechanism, as proposed for the aromatic hydroxylation of phenol by the homologous enzyme phenol hydoxylase.[5] The calculation of the hydroxylation step was performed by applying the reaction coordinate parameter $r = d(O_p–O_d) - d(O_d–C_{3'})$ as an approximation to the intrinsic reaction coordinate. This reaction coordinate was harmonically restrained (k = 5 000 kcal mol^{-1} $Å^{-2}$) using the CHARMM command RESDistance. By changing r in steps of 0.1 Å, from −1.8 Å, corresponding to the geometry of the reactants, to +1.2 Å, corresponding to the geometry of the products, the distal oxygen of the flavin cofactor was forced to move stepwise from the C4a-hydroperoxyflavin toward the substrate, corresponding to the process of hydroxylation. For each value of r, the active site region (i.e., the 10-Å sphere) was optimized to the same gradient tolerance used for the optimization of the initial geometry, requiring 60 to 250 steps of ABNR minimization. To prevent the water molecules in the optimized region from moving over large distances, which may cause undesired discontinuities along the reaction pathway, they were harmonically restrained to their initial (optimized) coordinates, using a small force constant of 5.0 kcal mol^{-1} $Å^{-2}$.

Other reaction coordinates could have been chosen for the simulation. The reaction coordinate used here ([i.e., $r = d(O_p–O_d) - d(O_d–C_{3'})$], is justified by the smooth and continuous form of the resulting path and the corresponding energy profile (see Results). Furthermore, the reaction coordinate was tested by performing the simulation in the reverse direction, using the same method but starting from the optimized product geometry. This yielded identical results.

The top of the energy profile represents the approximate transition state of the hydroxylation step in the reaction cycle. To determine this maximum more precisely, the energies of some additional points on the reaction coordinate were calculated, varying r in steps of 0.01 Å around the top in the energy profile. To analyze the QM/MM transition state geometry obtained, vibrational analysis of the QM part of the transition state was performed *in vacuo* using Spartan 5.1.[28] Charges on the quantum mechanical atoms within the electrostatic potential of the molecular mechanical atoms were obtained from the Mulliken analysis routine available in CHARMM.

It is useful to note that the closed shell AM1 method, which

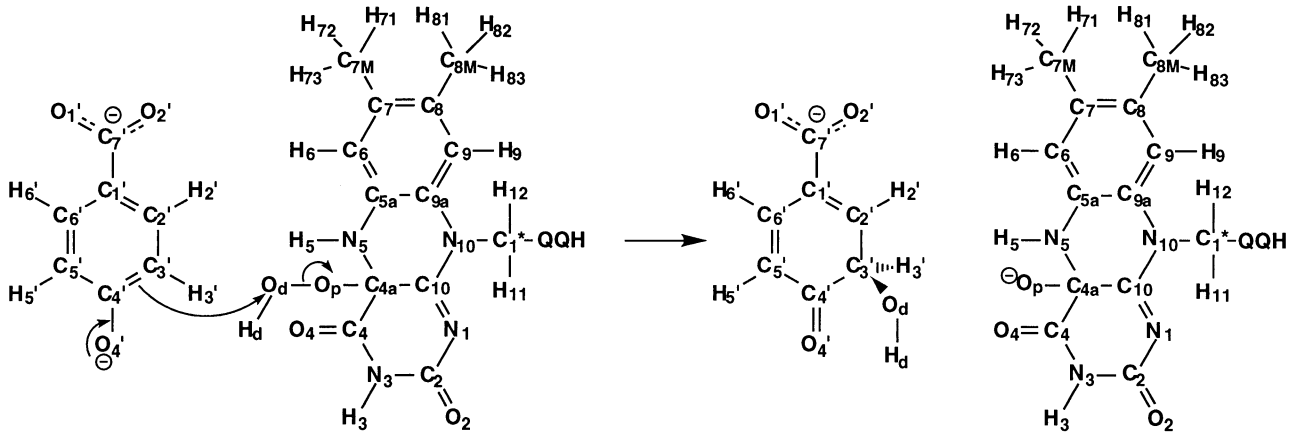

Figure 1. The hydroxylation of p*-hydroxybenzoate according to an electrophilic aromatic substitution mechanism and numbering of the atoms as used throughout the present paper.*

is used for the quantum mechanical region in the present model, cannot describe radical-type mechanisms. Therefore, the present study is not an attempt to answer definitely the discussion with respect to heterolytic cleavage versus homolytic cleavage of the peroxide oxygen–oxygen bond. However, the results are relevant for heterolytic bond dissociation reactions, such as the electrophilic aromatic substitution mechanism, which has been most recently supported by experimental evidence of the flavin-dependent monooxygenases.[5] Other limitations of the closed shell AM1 method are that AM1 has not been parameterized for unstable structures, such as transition states, and that possible interactions of the groundstate configuration with other electronic configurations are not taken into account. However, in spite of these limitations, the usefulness of AM1 in the present model is supported by a correlation of the resulting energy barriers with the logarithm of experimental rate constants for a series of fluorinated *p*-hydroxybenzoates.[18]

Frontier orbital analysis

Electronic details of the reaction mechanism described by the QM/MM model were obtained by analyzing the energies and density distributions of the four highest occupied molecular orbitals (HOMOs) and the four lowest unoccupied molecular orbitals (LUMOs) on the QM atoms for all reaction pathway geometries. The orbital density on a specific QM atom is defined as the sum of the squared molecular orbital coefficients for the contributions of the relevant atomic orbitals. The HOMO and LUMO density distributions represent nucleophilic and electrophilic reactivity, respectively, according to frontier orbital theory.[30] The molecular orbital energies and density distributions, were obtained from *in vacuo* single-point calculations of the geometries of the reaction pathway intermediates, using the AM1 method implemented in Spartan 5.1.

Amino acid decomposition analysis

To obtain qualitative information about the contribution of specific amino acids to the QM/MM energy barrier and to the energy difference between the reactants and products of the hydroxylation step, energy decomposition analyses were performed with a procedure similar to those used previously.[11,13,15] The analyses start from the energy difference between the reactants and the transition state, or the reactants and the products, without the MM protein environment. Then, one by one the amino acid residues are included in the QM/MM energy difference calculation in order of increasing distance between their center of mass (COM) and the distal oxygen of the hydroperoxyflavin. The effect of an (MM) amino acid on the QM/MM energy difference gives an approximate and qualitative indication of its influence on the hydroxylation step in the active site of PHBH. The results obtained from this analysis do not include dielectric screening and other solvation effects and therefore overestimate the effect of distant residues.[15] It should be clear that the analysis relates specifically to the hydroxylation step in the reaction cycle. The results, therefore, are not necessarily directly comparable to experimental studies on mutant enzymes in which effects on other steps as well as changes in protein structure can play a role.

RESULTS

Comparison of AM1, HF, and B3LYP results

Table 1 presents the results of the gas-phase calculations performed to validate the AM1 method for the relevant reactant and product molecules in the PHBH model. Although the peroxide O–O bond length in the C4a-hydroperoxyflavin appears to be somewhat underestimated by AM1, the other geometric variables involving the hydroperoxide moiety are in good agreement with the HF/6-31+G(d) and B3LYP/6-31+G(d) results. The differences in the C4a–O_p bond length and the C10-C4a-O_p angle between the C4a-hydroperoxyflavin and C4a-hydroxyflavin, as predicted by the B3LYP/6-31+G(d) method, are well reproduced by AM1. Furthermore, it is interesting to note that for most of the C–O bonds in the different compounds, the AM1 values are closer to the results from B3LYP/6-31+G(d) than to those from HF/6-31+G(d). The reasonable agreement between AM1 and B3LYP/6-31+G(d), which is the best level of theory used and includes electron correlation to a certain extent, supports the accuracy of AM1 for the QM system in the present QM/MM model.

QM/MM reaction pathway calculation for the hydroxylation reaction in *p*-hydroxybenzoate hydroxylase

Color Plate 1a presents the geometry of the active site region obtained by energy minimization of the initial model derived from the crystal structure, using the constraints and cutoffs as defined in Methods. The non-hydrogen atoms deviated from the initial coordinates, with a root-mean-squared difference (RMSD) of 0.44 Å. Table 2 shows that notable hydrogen bond interactions between the substrate and active site amino acids, which have been reported to be present in the crystal structures of PHBH in complex with *p*-hydroxybenzoate and 3,4-dihydroxybenzoate,[20] are preserved in the optimized model. An additional hydrogen bond is observed between the distal oxygen of C4a-hydroperoxyflavin and a water molecule (Wat717). The optimized structure represents the enzyme–C4a-hydroperoxyflavin–substrate complex in the PHBH reaction cycle and was used as the starting geometry for the reaction pathway calculation for the aromatic hydroxylation of the substrate. Figure 2 presents the energies of the calculated reaction pathway intermediates as a function of the reaction coordinate variable *r*, relative to the energy of the initial optimized geometry. The energy maximum is at $r = -0.54$. This point represents the transition state structure of the hydroxylation step (Color Plate 1b). Gas-phase normal mode analysis validates this transition state geometry by showing only one large negative eigenvalue corresponding to the transfer of the hydroxy group from the cofactor to the substrate, which is absent in the reactant and product geometries (results not shown). The energy barrier to the hydroxylation step is given by the difference between the energy of this transition state and the energy of the initial structure. This QM/MM calculated energy barrier of 17.6 kcal/mol is approximately 1.5 times higher than the experimental activation energy.[31] The last point on the reaction pathway ($r = 1.2$ Å) was further optimized, without the reaction coordinate distance restraint term. The resulting optimized product geometry (Color Plate 1c) remained almost identical to the last pathway geometry (RMSD = 0.03 Å) and contains

Table 1. A representative selection of bond lengths (Å), angles (degrees), dihedral angles (degrees), and energy differences (in kcal/mol) of AM1-, HF-, and B3LYP-optimized structures (in vacuum) of C4a-hydroperoxyflavin, *p*-hydroxybenzoate, C4a-peroxyflavin, and hydroxycyclohexadienone[a]

Parameter	AM1	HF/6-31+G(d)	B3LYP/6-31+G(d)
C4a–hydroperoxyflavin			
C_{4a}–O_p	1.484	1.425	1.486
O_p–O_d	1.280	1.385	1.444
C_{4a}–O_p–O_d	113.3	110.3	108.9
C_{10}–C_{4a}–O_p	103.2	102.7	102.2
C_{4a}–O_p–O_d–H_d	−82.9	−92.8	−84.6
C4a–hydroxyflavin			
C_{4a}–O_p	1.297	1.309	1.323
C_{10}–C_{4a}–O_p	109.9	108.5	108.5
p-Hydroxybenzoate			
$C_{1'}$–$C_{2'}$	1.402	1.399	1.410
$C_{2'}$–$C_{3'}$	1.382	1.385	1.396
$C_{3'}$–$C_{4'}$	1.438	1.434	1.443
$C_{4'}$–$O_{4'}$	1.279	1.266	1.291
$C_{1'}$–$C_{7'}$	1.497	1.522	1.531
$C_{7'}$–$O_{1'}$	1.276	1.247	1.273
Hydroxycyclohexadienone			
$C_{1'}$–$C_{2'}$	1.345	1.329	1.352
$C_{2'}$–$C_{3'}$	1.492	1.500	1.497
$C_{3'}$–$C_{4'}$	1.524	1.523	1.533
$C_{4'}$–$O_{4'}$	1.241	1.208	1.240
$C_{1'}$–$C_{7'}$	1.525	1.545	1.553
$C_{7'}$–$O_{1'}$	1.264	1.235	1.261
$C_{3'}$–$O_{d'}$	1.419	1.396	1.417
$O_{4'}$–$C_{4'}$–$C_{3'}$–O_d	−26.9	−27.3	−23.4
$\Delta E_{\text{products}-\text{reactants}}$[b]	−139.97	−130.94	−121.56

[a] Labels as in Figure 1.
[b] *Note:* An unusual large zero-point energy (ZPE) correction (+80 kcal/mol) for the energy difference was found at the HF/6-31+G(d) level, mostly due to a large ZPE difference between the C4a-hydroperoxyflavin and the C4a-hydroxyflavin. Although higher level frequency calculations would be required to test the validity of this large ZPE correction, it indicates that the enthalpy values may be significantly different from the energy values below. This also suggests that the AM1 results should be interpreted as energies rather than enthalpies.

deprotonated C4a-hydroxyflavin and a σ adduct of *p*-hydroxybenzoate. In this product of the calculated reaction pathway, the planar conformation of the $C_{3'}$ of the substrate is changed to a tetrahedral conformation as expected for the cyclohexadienone product shown in Figure 1.

Analysis of changes in charge distribution and bond distances along the reaction pathway

The atomic charges on the QM atoms in the reactant, transition state, and product geometries, including the effect of the protein, were obtained by performing a Mulliken analysis in CHARMM (Table 3). The changes in atomic charge are indicative of an electrophilic aromatic substitution-type mechanism (Figure 1). This especially follows from the total charges on the substrate ring and cofactor which reveal $-1e$ charge transfer from the substrate to the C4a-hydroxyflavin (Table 3). Table 4 presents the changes in bond distances and bond orders in the carbon ring of the substrate. Along the calculated reaction pathway, the bond orders of the $C_{1'}$–$C_{2'}$ bond and the $C_{5'}$–$C_{6'}$ bond increase, whereas the other bonds in the carbon ring become single bonds, demonstrating that the aromatic carbon ring has changed to a cyclohexadienone. Furthermore, the decrease in charge on $O_{4'}$ (Table 3) and the increase in $C_{4'}$–$O_{4'}$ bond order (Table 4) are in agreement with the formation of a carbonyl group at the para position.

Changes in the orientation of active site amino acids

The RMSD for nonhydrogen atoms between the optimized coordinates of subsequent pathway geometries stayed within 0.05 Å, indicating that only small changes in the conformation of the optimized atoms in the active site occur along the reaction coordinate. The small structural changes occur especially at three sites in the optimized region. First, Ser212, Arg214, and Tyr222, which form the binding site for the carboxylate moiety of the substrate, adapt their orientation in response to a small rotation of the substrate. As a result, the four hydrogen bonds between the carboxylate moiety of the substrate and these amino acid residues are well preserved along the reaction coordinate (Table 2). Second, Tyr201 and

Table 2. Hydrogen bond distances between active site amino acids and the substrate in the reactants (*p*-hydroxybenzoate–C4a-hydroperoxyflavin), the transition state ($r = -0.54$), and the products (cyclohexadienone–C4a-hydroxyflavin)[a]

Hydrogen bond (Å) amino acid–substrate	Reactants	Transition state	Products
Ser212-H–$O_{1'}$	2.06	2.03	1.97
Arg214-H–$O_{1'}$	1.82	1.81	1.80
Arg214-H–$O_{2'}$	1.94	1.89	1.83
Tyr222-H–$O_{2'}$	1.96	1.93	1.92
Tyr201-H–$O_{4'}$	1.89	1.93	2.10
Pro293=O–H_d	2.35	1.98	2.42
Wat717-H–O_p	2.20	2.11	2.01
Wat717-H–O_d	2.16	3.14	4.01

[a] Substrate atom labels as in Figure 1.

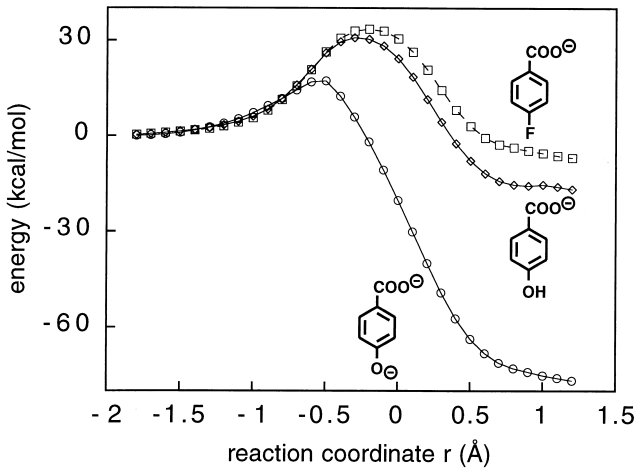

Figure 2. QM/MM reaction pathway energy profiles of the hydroxylation of p*-hydroxybenzoate in its dianionic and monoanionic form and of the effector* p*-fluorobenzoate, as a function of the reaction coordinate* $r = d(O_p–O_d) - d(O_d–C_{3'})$. *Energies are given relative to the reactants.*

Tyr385, which form a hydrogen-bonding network to stabilize the deprotonated hydroxyl moiety of the substrate, also adapt to the movement of the substrate. Notably, the hydrogen bond distance between the hydroxyl proton of Tyr201 and $O_{4'}$ of the substrate increases along the reaction coordinate from 1.89 to 2.10 Å (Table 2). The third movement is observed around the peptide bond between Pro293 and Thr294. Toward the transition state, this part of the backbone shows a small rotation. Because of this rotation, the carbonyl group of Pro293 points toward H_d of the hydroperoxyflavin and interacts with the O_d–H_d moiety in the process of being transferred to the substrate (Color Plate 1b, Table 2). At the end of the reaction pathway this carbonyl group rotates back to its original position.

In the crystal structure, Wat717 is hydrogen bonded to the backbone nitrogen of Gly298. On minimization of the present model, in which oxidized flavin is replaced by C4a-hydroperoxyflavin, this water molecule forms a hydrogen bond with the peroxide moiety of the cofactor. As the reaction proceeds, this interaction between Wat717 and the proximal oxygen of the peroxide becomes stronger (Table 2).

Activation of the substrate

In the model described above, the hydroxyl moiety at the $C_{4'}$ position of the substrate is deprotonated. This deprotonation is proposed to activate the substrate for the nucleophilic attack on the cofactor.[3] To investigate the importance of deprotonation, similar reaction pathway calculations were performed for the aromatic hydroxylation of the protonated substrate and of the effector *p*-fluorobenzoate, in which the hydroxyl moiety is replaced by a fluorine substituent. Figure 2 shows that the energy barriers obtained for these two substrate analogues are a factor of 2 higher than for the native substrate. On the basis of the correlation between the calculated energy barriers and the logarithm of experimental rate constants of conversion of a series of fluorinated substrates[18] these barriers would correspond to a rate constant of about 0.01 s^{-1}. Thus, these results support the proposal that deprotonation of the *p*-hydroxybenzoate substrate is essential for the hydroxylation reaction. They are also in agreement with the experimental observation that with *p*-fluorobenzoate hydroxylation does not proceed, although *p*-fluorobenzoate binds to the active site of PHBH and initiates reduction of the flavin and formation of the C4a-hydroperoxyflavin.

To obtain more detailed insight into the reaction process the changes in energy and distribution of the molecular orbitals involved were analyzed. Since the analysis of the AM1 orbitals does not include the effects of the protein it is only expected to give a qualitative picture of the changes along the reaction coordinate. Figure 3a presents the energies of the four highest occupied orbitals (HOMOs) and the four lowest unoccupied orbitals (LUMOs), as functions of the reaction coordinate, for the model with deprotonated substrate. This so-called Walsh diagram can be interpreted in terms of frontier orbital theory. In the initial cofactor substrate complex the HOMO and LUMO frontier orbitals are energetically separated from the other occupied and unoccupied orbitals. Furthermore, the HOMO is fully localized on the *p*-hydroxybenzoate (graphically presented in Color Plate 2a) which is in accordance with its role as nucleophile in the hydroxylation reaction, whereas the LUMO is localized on the C4a-hydroperoxyflavin in line with its role as electrophile. As the reaction proceeds the HOMO and LUMO orbitals interact, which results in a decrease in the HOMO energy and an increase in the LUMO energy (Figure 3a). Meanwhile, the HOMO density gradually moves from the substrate to the cofactor (Figure 3b and c) and the LUMO density moves from the cofactor to the substrate (see Discussion).

For comparison, Figure 3b shows the Walsh diagram for the calculated reaction pathway with protonated substrate. In this case, the HOMO, HOMO-1, and HOMO-2 are all located around the carboxylate moiety of the substrate and have no density on the reacting $C_{3'}$ atom. Analysis of the orbital distributions indicates that the HOMO-3, which initially has density on $C_{3'}$, is the true interacting orbital. Comparison of Figure 3a and b shows that the energy gap between the interacting HOMO-3 and LUMO for the reaction with protonated substrate (7.7 eV) is almost twice as large as the energy gap between the interacting HOMO and LUMO for the reaction with unproto-

Table 3. Atomic charge distribution in the reactants, transition state, and products according to Mulliken analysis of the QM/MM model[a]

Atom	Reactants	Transition state	Products	Atom	Reactants	Transition state	Products
N_1	−0.326	−0.343	−0.359	$C_{1'}$	−0.319	−0.282	−0.129
C_2	0.384	0.386	0.394	$C_{7'}$	0.388	0.389	0.382
O_2	−0.323	−0.342	−0.374	$O_{1'}$	−0.699	−0.691	−0.612
N_3	−0.377	−0.384	−0.386	$O_{2'}$	−0.716	−0.704	−0.691
H_3	0.317	0.307	0.286	$C_{2'}$	−0.020	−0.019	−0.030
C_4	0.324	0.312	0.273	$H_{2'}$	0.112	0.123	0.167
O_4	−0.336	−0.355	−0.430	$C_{6'}$	−0.047	−0.007	−0.136
C_{4a}	0.132	0.197	0.307	$H_{6'}$	0.077	0.091	0.135
O_p	−0.190	−0.375	−0.665	$C_{3'}$	−0.312	−0.288	−0.245
O_d	−0.228	−0.132	−0.331	$H_{3'}$	0.132	0.140	0.173
H_d	0.291	0.237	0.260	$C_{5'}$	−0.398	−0.356	0.005
N_5	−0.280	−0.282	−0.310	$H_{5'}$	0.105	0.115	0.122
H_5	0.305	0.281	0.222	$C_{4'}$	0.285	0.291	0.250
C_{5a}	0.064	0.066	0.090	$O_{4'}$	−0.556	−0.526	−0.323
C_6	−0.134	−0.146	−0.183				
H_6	0.207	0.195	0.146	Total substrate:	−1.969	−1.725	−0.933
C_7	−0.068	−0.070	−0.069				
C_{7M}	−0.174	−0.173	−0.169				
H_{71}	0.084	0.081	0.082	Total flavin–O_p:	−0.094	−0.380	−0.997
H_{72}	0.103	0.099	0.086				
H_{73}	0.054	0.053	0.049				
C_8	−0.090	−0.099	−0.116	Total O_d–H_d:	0.063	0.105	−0.071
C_{8M}	−0.176	−0.174	−0.170				
H_{81}	0.081	0.079	0.072				
H_{82}	0.088	0.087	0.086				
H_{83}	0.086	0.083	0.079				
C_9	−0.149	−0.149	−0.151				
H_9	0.120	0.118	0.113				
$C9_a$	−0.007	−0.006	0.009				
N_{10}	−0.185	−0.191	−0.198				
C_{10}	0.180	0.179	0.131				
C_{1*}	−0.076	−0.072	−0.077				
H_{11}	0.060	0.054	0.045				
H_{12}	0.113	0.112	0.108				
QQH	0.096	0.093	0.085				

[a] Atom labeling as in Figure 1.

nated substrate (4.3 eV), which is in line with the difference in energy barrier observed.

Activation of the cofactor

Figure 4a and b presents the changes in bond distances, along the calculated reaction pathway, of the bonds included in the present reaction coordinate, i.e., the bond to be broken, O_p–O_d, and the bond to be formed, O_d–$C_{3'}$. Figure 4a and b shows a notable feature of the approximate reaction pathway model. Following the initial approach of O_d and $C_{3'}$, from O_d–$C_{3'}$ = 3.0 to 2.0 Å, elongation of the O_p–O_d bond is observed. This elongation occurs prior to the further shortening of the O_d–$C_{3'}$ distance (from 2.0 to 1.4 Å), corresponding to the actual O_d–$C_{3'}$ bond formation. The lengthening of the peroxide oxygen–oxygen bond might be rationalized through analysis of the changes in the distribution of the LUMO in the substrate–cofactor complex. Figure 4c shows that the LUMO, initially located on the flavin ring, has no density on the atom that actually attacks the substrate, i.e., at the distal oxygen (O_d) of the peroxide moiety. The analysis of the LUMO distribution along the reaction pathway shows that this expected LUMO density at the distal oxygen occurs at an intermediate phase in the reaction where $-0.6 \leq r \leq -0.2$. Figure 4b shows that the most effective lengthening of the peroxide bond occurs at $-0.6 \leq r \leq -0.4$. A comparison of Figure 4b and c suggests that the early lengthening of the peroxide oxygen–oxygen bond in the reaction pathway is related to the increase in LUMO density on O_d. The subsequent interaction with the HOMO on the substrate $C_{3'}$ on the distal oxygen may then lead to the

Table 4. Bond lengths (Å) and bond orders[a] in the reactants (*p*-hydroxybenzoate–C4a-hydroperoxyflavin), the transition state ($r = -0.54$), and the products (cyclohexadienone–C4a-hydroxyflavin)[b]

	Bond length (Å)			Bond order		
Bond	Reactants	Transition state	Products	Reactants	Transition state	Products
O_p–O_d	1.28	1.52	2.96	1.03	0.71	0.00
O_d–C_3	3.09	2.06	1.41	0.01	0.21	1.01
$C_{1'}$–$C_{2'}$	1.40	1.38	1.35	1.39	1.51	1.82
$C_{2'}$–$C_{3'}$	1.38	1.41	1.49	1.44	1.27	0.97
$C_{3'}$–$C_{4'}$	1.44	1.45	1.52	1.14	1.10	0.90
$C_{4'}$–$C_{5'}$	1.44	1.45	1.46	1.12	1.08	1.00
$C_{5'}$–$C_{6'}$	1.37	1.36	1.35	1.54	1.62	1.78
$C_{6'}$–$C_{1'}$	1.41	1.42	1.45	1.30	1.22	1.06
$C_{4'}$–$O_{4'}$	1.27	1.27	1.24	1.53	1.57	1.84

[a] Data from Ref. 28.
[b] Atom labels as in Figure 1.

formation of the $C_{3'}$–O_d bond. It should be noted that the equilibrium peroxide oxygen–oxygen bond calculated by AM1 is about 0.16 Å shorter than the bond length obtained at the B3LYP/6-31+G(d) level and that the orbital contributions predicted by AM1 are slightly different from those predicted at higher levels. Furthermore, the true reaction may involve interactions of the groundstate configuration with other electronic configurations that are not included in the present model. The effect of lengthening the peroxide O–O bond on the LUMO density at O_d should therefore be interpreted in a qualitative manner only.

The role of active site amino acids in the hydroxylation

Figure 5 presents the results of the energy decomposition analyses, which indicate approximately the effects of active site amino acids and water molecules on the hydroxylation step. In Figure 5a, the QM/MM energy difference between the reactants and transition state structures of the present reaction pathway is plotted as a function of the amino acid residues included (in order of the distance between their center of mass, COM, and the distal oxygen of hydroperoxyflavin). Similarly, Figure 5b presents the QM/MM energy difference between the reactant and the product structures of the present reaction pathway as a function of the residues included.

Some residues with a significant effect on the QM/MM energy differences are labeled. Analysis of the different contributions to the QM/MM energies indicates that these strong effects of individual residues on the QM/MM energy are largely due to electrostatic interactions between the QM and MM atoms. Most of these residues, except for Tyr201, Pro293, and Asn300, are charged residues. For example, Arg214 is involved in binding the carboxylate moiety of the substrate[20] and Arg44 forms a hydrogen bond with the negatively charged phosphate oxygen of the AMP moiety of the FAD cofactor.[20] All these charged residues influence the electrostatic field in which a net charge transfer of $-1e$ from the substrate to the cofactor occurs along the reaction coordinate. These electrostatic contributions either favor or disfavor the reaction depending on the charge and the position of the residue relative to the reactive (QM) atoms.

Neutral amino acid residues may influence the energy differences, presented in Figure 5, through steric or dipole interactions and hydrogen bonds. For example, Figure 5a indicates that Tyr201 increases the energy barrier. The role of Tyr201 in the present pathway model, which represents only one particular step in the reaction cycle, is to stabilize the negative charge on the deprotonated hydroxyl moiety of the substrate, via a hydrogen bond, in the C4a-hydroperoxyflavin substrate complex. As the reaction proceeds this oxyanion formally becomes a carbonyl oxygen, which is less charged, and therefore the hydrogen bond with the tyrosine residue weakens. This effect is also reflected by the increase in the hydrogen bond distance between Tyr201 and $O_{4'}$ of the substrate along the reaction coordinate (Table 2).

As already mentioned on the basis of Table 2, the hydrogen bond distance between crystal water 717 and the proximal oxygen of the cofactor decreases along the reaction coordinate. Figure 5a and b indicates a stabilizing effect of Wat717 on the transition state and the products relative to the reactants. This is clearly due to the increasing interaction of Wat717 with the proximal oxygen of the peroxide moiety which becomes more negatively charged as the reaction proceeds (Table 3).

Perhaps the most interesting observation to be made in comparing Figure 5a and b is that Pro293 decreases the energy barrier (Figure 5a), while it has almost no effect on the overall energy difference between reactants and products (Figure 5b). In the transition state of the reaction pathway model, the backbone carbonyl moiety of Pro293 is in close proximity to the H_d atom of the peroxide moiety (Table 2), which is being transferred from the peroxide cofactor to the substrate. In this transition state geometry, the O_p–O_d bond has been partially broken (Table 4, Color Plate 1b) and the total charge on the (somewhat isolated) OH moiety has become more positive ($0.11e$, by Mulliken analysis, Table 3). The OH moiety appears to be stabilized by the interaction with the partial negative charge of -0.55 on the carbonyl oxygen of Pro293. This

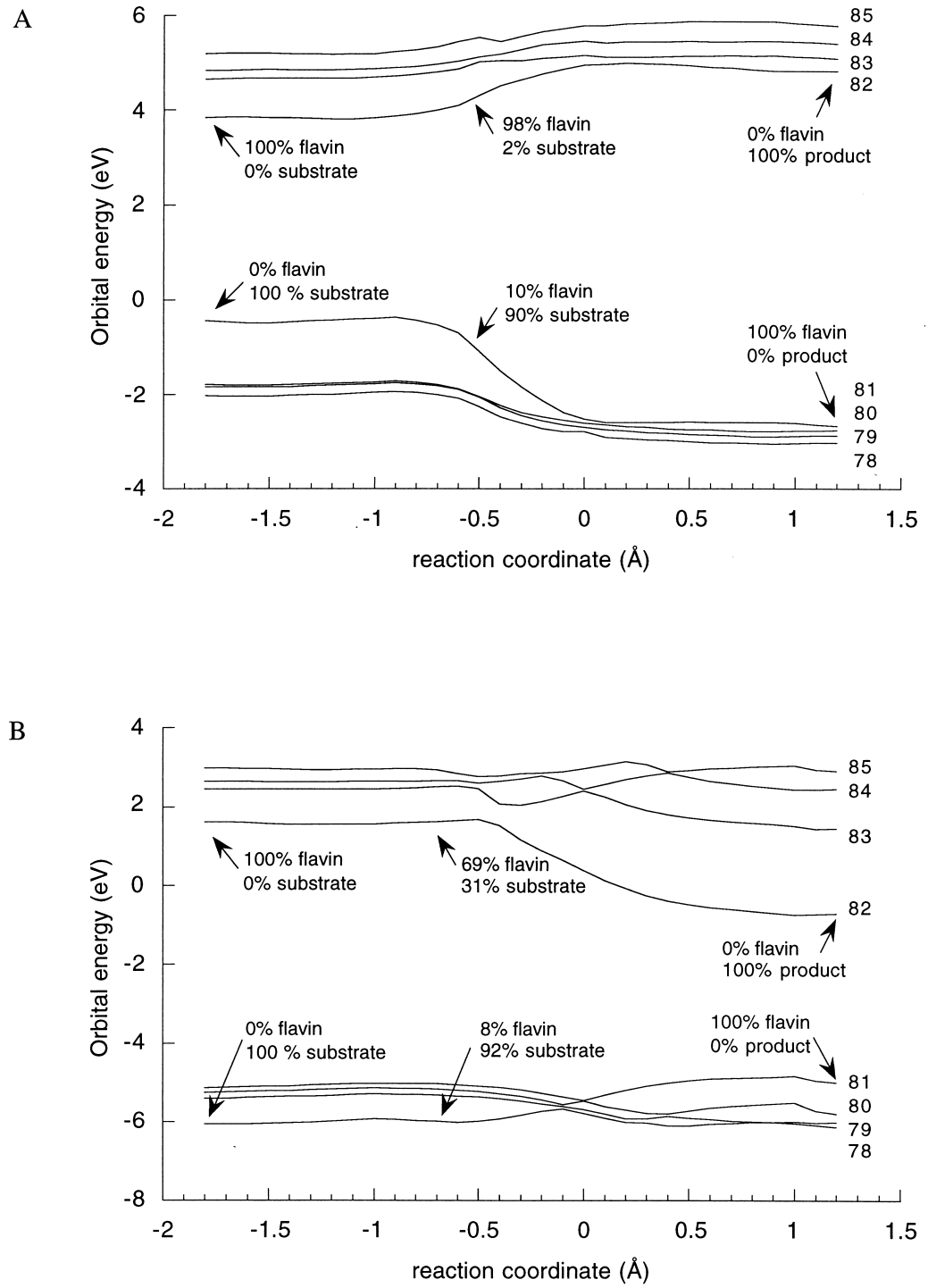

Figure 3. Walsh diagrams, showing the energies of orbitals 78–85, i.e., from HOMO-3 to LUMO+3, as a function of the reaction coordinate for (a) hydroxylation of deprotonated substrate and (b) protonated substrate. The density distributions of the interacting HOMO and LUMO orbitals are represented as percentages on substrate and cofactor.

favorable electrostatic interaction is not (or less) present in the reactant and product geometries of the present reaction pathway (Table 2). Thus, the backbone carbonyl moiety of Pro293 appears to be responsible for a specific stabilization of the transition state of the hydroxylation process.

It is interesting to note that, despite the fact that the most significant effects of individual residues have an electrostatic character, the total effect of all electrostatic interactions of the reacting QM system with the protein almost cancel out. The other contributions to the QM/MM energy differences, i.e., the QM/MM van der Waals interactions and the purely MM energy terms, account for 1.8 kcal/mol stabilization of the transition state and 3.6 kcal/mol stabilization of the products, relative to the reactants.

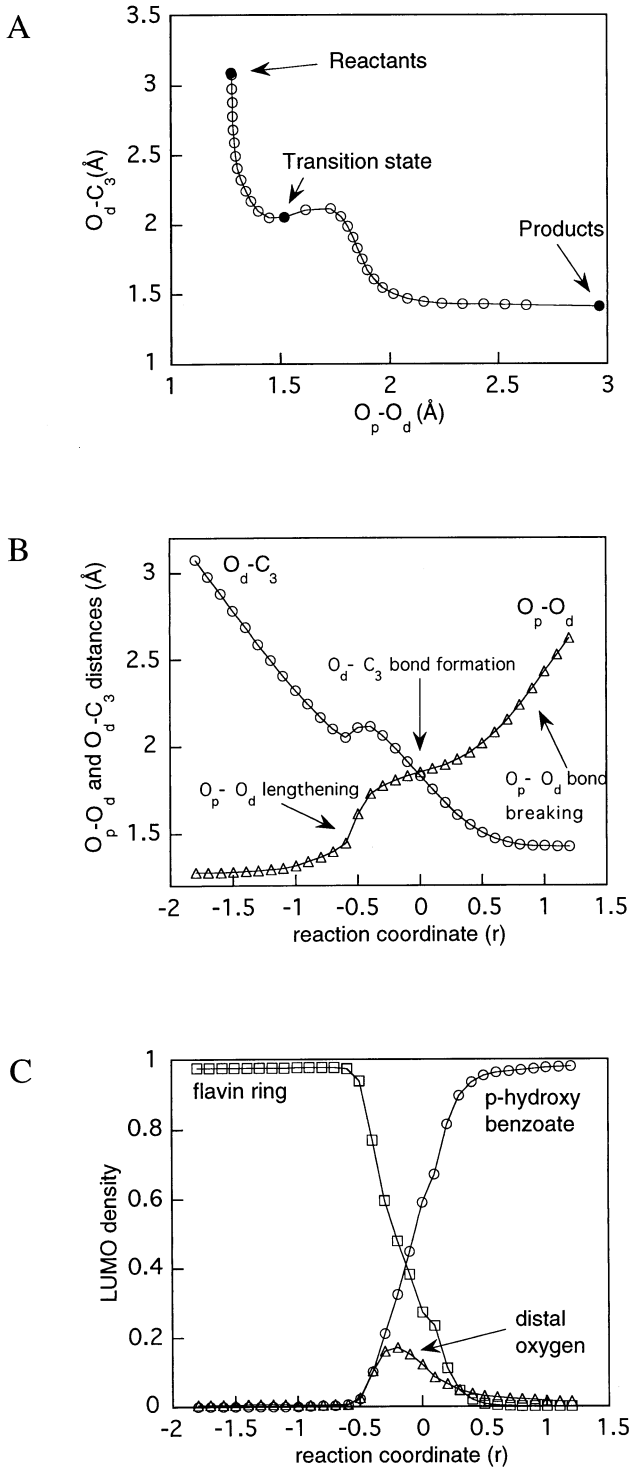

Figure 4. (a) The O_d–$C_{3'}$ distance (forming bond) versus the O_p–O_d distances (breaking bond). The closed circles correspond to the reactant state (left top), the transition state, and the product state (right bottom). (b) The change in O_p–O_d and O_d–$C_{3'}$ atomic distance as a function of the reaction coordinate r. *(c) The LUMO densities on the substrate, flavin ring, and distal oxygen as a function of the reaction coordinate* r, *obtained by* in vacuo *single-point calculations (AM1) of the geometries of the QM atoms obtained in the QM/MM reaction pathway calculation with dianionic* p*-hydroxybenzoate.*

DISCUSSION

The hydroxylation step in the reaction cycle of flavin-dependent aromatic hydroxylases has been suggested to proceed via an electrophilic aromatic substitution mechanism.[5] The present QM/MM reaction pathway calculations provide a model for this reaction step. Analysis of the charge distribution and the bond lengths along the reaction coordinate of this model for the hydroxylation step are in line with an electrophilic aromatic substitution type of mechanism and support the formation of a hydroxycyclohexadienone as the initial reaction product (Tables 3 and 4). This hydroxycyclohexadienone may represent the so-called intermediate II observed in stopped flow studies with phenol hydroxylase.[5]

Additional results of the reaction pathway analysis provide insight into the role of substrate and cofactor activation in catalysis by PHBH. Deprotonation of the hydroxyl moiety of the substrate has previously been proposed to lead to activation of the $C_{3'}$ atom toward a nucleophilic attack on the cofactor, which is essential for the hydroxylation step.[1,2] The results of the present reaction pathway calculations, performed for both protonated and deprotonated substrate, further strengthen the proposed mechanism for substrate activation by showing that this deprotonation of the hydroxyl moiety leads to a significantly lower energy barrier for the hydroxylation reaction, corresponding to a 4×10^3-fold increase in the rate of hydroxylation. Furthermore, results obtained with protonated *p*-hydroxybenzoate appear to be comparable to results obtained with 4-fluorobenzoate. 4-Fluorobenzoate is known to bind to the active site and to stimulate formation of the C4a-hydroperoxyflavin intermediate,[32] without subsequently being hydroxylated. This observation has been used as an argument to indicate the importance of substrate activation, which is impossible with the 4-fluorobenzoate lacking the hydroxyl moiety at $C_{4'}$. The similarity observed between the reaction pathways obtained with the protonated substrate and 4-fluorobenzoate suggests that 4-fluorobenzoate is indeed a good model for an unactivated substrate.

In addition to substrate activation, activation of the C4a-hydroperoxyflavin cofactor for the hydroxylation reaction is of interest. Maeda-Yorita and Massey[5] and Vervoort et al.[33] suggested that protonation of the distal oxygen is required for electrophilic reactivity of the peroxide moiety of the flavin cofactor intermediate. However, this protonation by itself appears insufficient to activate the cofactor, since virtually no LUMO density is present on the distal oxygen in the optimized substrate–C4a-hydroperoxyflavin complex. This illustrates that the electronic properties of the C4a-hydroperoxyflavin molecule are not completely characterized by its calculated equilibrium groundstate. The results suggest that an early lengthening of the O–O bond, accompanied by an increase in LUMO density at the protonated distal oxygen, enhances the C–O bond formation and the reaction to proceed. Since the reaction coordinate is an approximation to the intrinsic reaction coordinate and does not provide a dynamic description of the reaction, the question of how this lengthening actually proceeds remains open for discussion. Peroxide oxygen–oxygen bonds are relatively weak (with small force constants for the O–O stretching),[34] which implies that an oxygen–oxygen lengthening of 0.2–0.3 Å can be expected to occur at low vibrational levels and at physiological temperatures.

It is interesting that the variation in the energy barriers

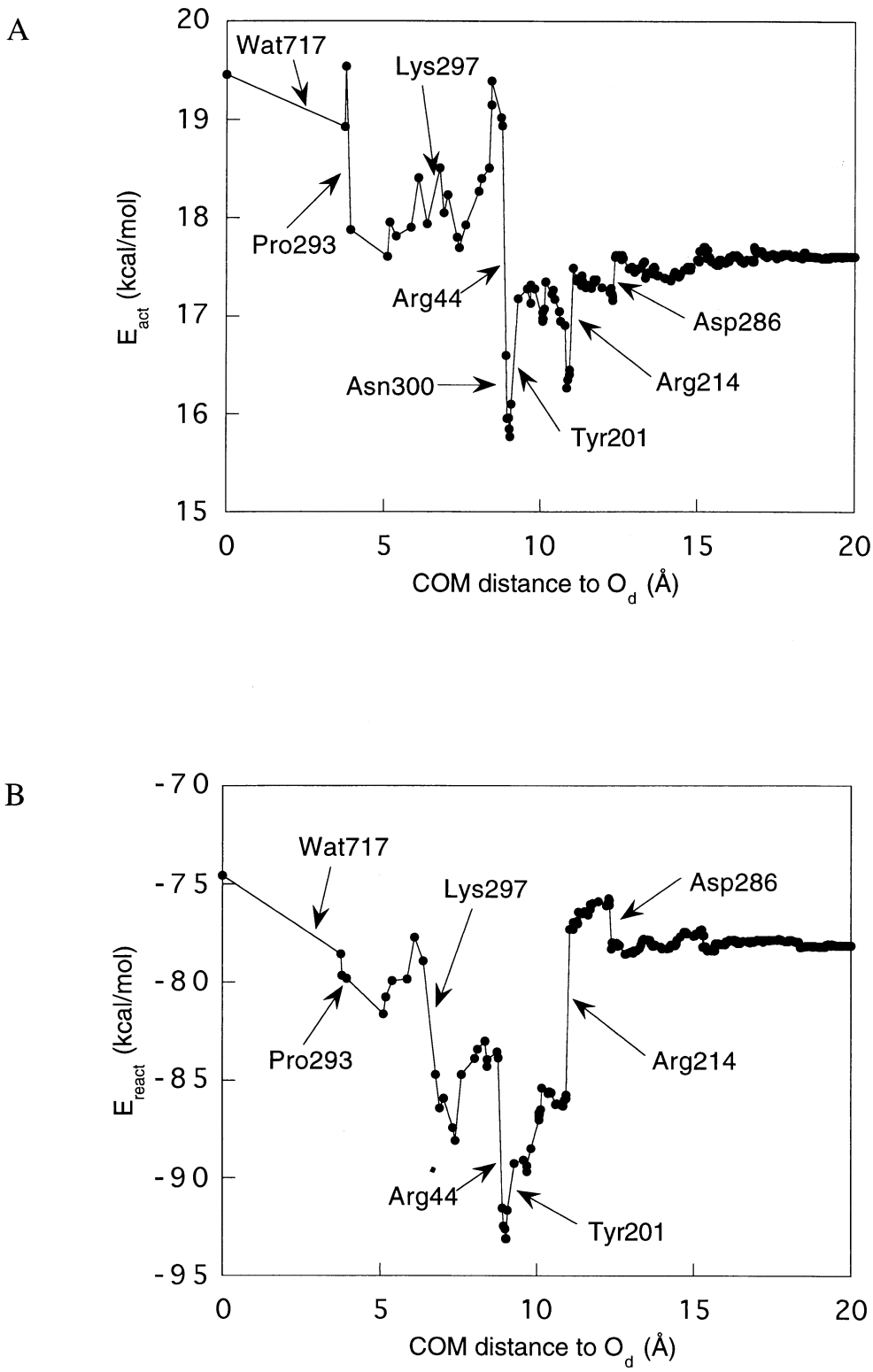

Figure 5. Amino acid decomposition analysis illustrating the effect of nonbonded van der Waals and electrostatic interactions between protein residues and the substrate–flavin complex on the difference in the QM/MM energy term between (a) the reactants and the transition state and (b) the reactants and products of the present reaction pathway.

appears to depend on the relative stability of the reactants and products, rather than on specific interactions in the transition state (Figure 2). A similar conclusion can be drawn from a previous study showing a linear correlation of calculated differences in heats of formation between the *p*-hydroxybenzoate and the hydroxycyclohexadienone with the natural logarithm of the experimental rate constants for the overall conversion of a series of fluorinated substrates.[35] The energy differences of

−78 kcal/mol between reactants and products, obtained in the present QM/MM calculation for deprotonated substrate, would suggest this step to be exothermic in the context of the overall reaction cycle. However, since no experimental reaction enthalpy is available for the individual hydroxylation step to validate this value, it may not be interpreted in an absolute way. The energy decomposition analysis (Figure 5b) indicates that the overall effect of the protein on the energy of the reaction may be relatively small and that the largest contribution comes from the QM system only. Comparison of AM1 with higher level calculations on the reactants and products in vacuum (Table 1) shows that AM1 overestimates the difference in energy of the reactants and products by about 20%. Furthermore, as also indicated in the note to Table 1, the QM energy difference may not be interpreted as enthalpy difference in an absolute way.

An important observation from the amino acid decomposition analysis is that the backbone carbonyl oxygen atom of Pro293 functions as a hydrogen bond acceptor for the hydrogen on the distal oxygen of the hydroperoxyflavin, specifically in the transition state geometry, which results in a lowering of the activation barrier. Proline residues, because of their cyclic structure, have a pronounced influence on backbone conformation. The presence of two neighboring proline residues, at positions 292 and 293, may indicate that a specific backbone orientation is essential in this part of the protein structure. In relation to the present results it is tempting to speculate that the presence of the proline residues and their specific effect on the backbone orientation contributes to the catalytic effect of the backbone carbonyl of Pro293 on the hydroxylation step.

Further results of the residue analysis indicate that Tyr201 stabilizes the substrate in an activated deprotonated state. It should be noticed that the essential role of Tyr201 in catalysis, as experimentally determined by mutating it to a phenylalanine, is to enhance the deprotonation of the enzyme bound substrate.[3,4] This deprotonation process is not included in the present reaction coordinate and, therefore, in the present reaction pathway, the only effect of Tyr201 is to increase the activation barrier because it stabilizes the reactant state more than the transition state.

The crystal water 717 has a driving effect on the hydroxylation reaction in the present model. It stabilizes the increasing negative charge on the proximal oxygen of the cofactor as the reaction proceeds. At the end of this reaction step, this water is would be in a good position to be possibly involved in protonation of this oxygen.

Overall, the enzyme lowers the energy barrier of the calculated reaction pathway for hydroxylation by only 1.8 kcal/mol. This value, obtained by comparing the barrier for the whole system with the barrier for the QM atoms alone (Figure 5b), is an approximate and qualitative indication of the catalytic effect of the enzyme on the hydroxylation step in the reaction cycle. Nevertheless, it indicates that the stabilization of the transition state in the hydroxylaton step by PHBH could be relatively small. Altogether, the present results corroborate the idea that the catalytic mechanism of the hydroxylation step by PHBH is mainly based on activating the substrate and cofactor. More specifically, the role of the enzyme appears to be to provide an environment that enables the coexistence of the activated deprotonated substrate (e.g., through the hydrogen bond of Tyr201) and the protonated C4a-hydroperoxyflavin, in the right orientation. The subsequent hydroxylation reaction, via an electrophilic attack of the cofactor on the substrate, readily proceeds, apparently with a small additional stabilization of the transition state, e.g., by Pro293.

ACKNOWLEDGMENTS

This work was supported by The Netherlands Organization for Scientific Research (NWO). A.J.M. is an EPSRC Advanced Research Fellow, and was previously a Wellcome Trust International Prize Travelling Research Fellow (Grant 041229). We thank Prof. Martin Karplus for his support and we acknowledge the referees for their useful comments on the manuscript.

REFERENCES

1 Vervoort, J., Rietjens, I.M.C.M., Van Berkel, W.J.H., and Veeger, C. Frontier orbital study on the 4-hydroxybenzoate-3-hydroxylase-dependent activity with benzoate derivatives. *Eur. J. Biochem.* 1992, **206,** 479–484

2 Entsch, B., Ballou, D.P., and Massey, V. Flavin–oxygen derivatives involved in hydroxylation by *p*-hydroxybenzoate hydroxylase. *J. Biol. Chem.* 1976, **251,** 2550–2563

3 Entsch, B., Palfey, B.A., Ballou, D.P., and Massey, V. Catalytic function of tyrosine residues in *p*-hydroxybenzoate hydroxylase as determined by the study of site-directed mutants. *J. Biol. Chem.* 1991, **266,** 17341–17349

4 Eschrich, K., Van Der Bolt, F.J.T., De Kok, A., and Van Berkel, W.J.H. Role of Tyr201 and Tyr385 in substrate activation by *p*-hydroxybenzoate hydroxylase from *Pseudomonas fluorescens*. *Eur. J. Biochem.* 1993, **216,** 137–146

5 Maeda-Yorita, K., and Massey, V. On the reaction mechanism of phenol hydroxylase: New information obtained by correlation of fluorescence and absorbance stopped flow studies. *J. Biol. Chem.* 1993, **268,** 4134–4144

6 Husain, M., Entsch, B., Ballou, D.P., Massey, V., and Chapman, J.P. Fluoride elimination from substrates in hydroxylation reactions catalyzed by *p*-hydroxybenzoate hydroxylase. *J. Biol. Chem.* 1980, **255,** 4189–4197

7 Keum, S.R., Gregory, D.H., and Bruice, T.C. Oxidation of aminophenols by 4α-hydroperoxy-5-ethyllumiflavin anion: Flavoenzyme hydroxylase mechanism. *J. Am. Chem. Soc.* 1990, **112,** 2711–2715

8 Anderson, R.F., Patel, K.B., and Stratford, M.R.L. Absorption spectra of substrates for *p*-hydroxybenzoate hydroxylase following electrophilic attack of the · OH radical in the 3 position. *J. Biol. Chem.* 1987, **262,** 17475–17479

9 Anderson, R.F., Patel, K.B., and Vojnovic, B. Absorption spectra of radical forms of 2,4-dihydroxybenzoic acid, a substrate for *p*-hydroxybenzoate hydroxylase. *J. Biol. Chem.* 1991, **266,** 13086–13090

10 Peräkylä, M., and Pakkanen, T.A. *Ab initio* models for receptor–ligand interactions in proteins. 3. Model assembly study of the proton transfer in the hydroxylation step of the catalytic mechanism of *p*-hydroxybenzoate hydroxylase. *J. Am. Chem. Soc.* 1993, **115,** 10958–10963

11 Bash, P.A., Field, M.J., Davenport, R.C., Petsko, G.A., Ringe, D., and Karplus, M. Computer simulation and analysis of the reaction pathway of triosephosphate isomerase. *Biochemistry* 1991, **30,** 5826–5832

12 Hartsough, D.S., and Merz, K.M. Dynamic force field models: Molecular dynamics simulations of human carbonic anhydrase II using a quantum mechanical/molecular mechanical coupled potential. *J. Phys. Chem.* 1995, **99,** 11266–11275
13 Cunningham, M.A., Ho, L.L., Nguyen, D.T., Gillilan, R.E., and Bash, P.A. Simulation of the enzyme reaction mechanism of malate dehydrogenase. *Biochemistry* 1997, **36,** 4800–4816
14 Harrison, M.J., Burton, N.A., and Hillier, I.H. Catalytic mechanism of the enzyme papain: Predictions with a hybrid quantum mechanical/molecular mechanical potential. *J. Am. Chem. Soc.* 1997, **119,** 12285–12291
15 Mulholland, A.J., and Richards, W.G. Acetyl-CoA enolization in citrate synthase: A quantum mechanical/molecular mechanical (QM/MM) study. *Proteins* 1997, **27,** 9–25
16 Mulholland, A.J., and Karplus, M. Computer modelling of biological molecules. *Biochem. Soc. Trans.* 1996, **24,** 247–254
17 Field, M.J., Bash, P.A., and Karplus, M. A combined quantum mechanical and molecular mechanical potential for molecular dynamics simulations. *J. Comp. Chem.* 1990, **11,** 700–733
18 Ridder, L., Mulholland, A.J., Vervoort, J., and Rietjens, I.M.C.M. Correlation of calculated activation energies with experimental rate constants for an enzyme catalyzed aromatic hydroxylation. *J. Am. Chem. Soc.* 1998, **120,** 7641–7642
19 Wierenga, R.K., De Jong, R.J., Kalk, K.H., Hol, W.G.J., and Drenth, J. Crystal structure of *p*-hydroxybenzoate hydroxylase. *J. Mol. Biol.* 1979, **131,** 55–73
20 Schreuder, H.A., Prick, P.A.J., Wierenga, R.K., Vriend, G., Wilson, K.S., Hol, W.G.J., and Drenth, J. Crystal structure of the *p*-hydroxybenzoate hydroxylase–substrate complex refined at 1.9 A° resolution: Analysis of the enzyme–substrate and enzyme–product complexes. *J. Mol. Biol.* 1989, **208,** 679–696
21 Schreuder, H.A., Van der Laan, J.M., Hol, W.G.J., and Drenth, J. The structure of *p*-hydroxybenzoate hydroxylase. In: *Chemistry and Biochemistry of Flavoproteins* (Müller, F., ed.). CRC Press, Boca Raton, Florida, 1991.
22 Schreuder, H.A., Hol, W.G.J., and Drenth, J. Analysis of the active site of the flavoprotein *p*-hydroxybenzoate hydroxylase and some ideas with respect to its reaction mechanism. *Biochemistry* 1990, **29,** 3101–3108
23 Vervoort, J., Müller, F., Lee, J., Moonen, C.T.W., and Van den Berg, W.A.M. Identifications of the true carbon-13 NMR spectrum of the stable intermediate II in bacterial luciferase. *Biochemistry* 1986, **25,** 8062–8067
24 Brooks, B.R., Bruccoleri, R.E., Olafson, B.D., States, D.J., Swaminathan, S., and Karplus, M. CHARMm: A program for macromolecular energy, minimization and dynamics calculations. *J. Comp. Chem.* 1983, **4,** 187–217
25 Dewar, M.J.S., Zoebisch, E.G., Healy, E.F., and Stewart, J.J.P. AM1: A new general purpose quantum mechanical molecular model. *J. Am. Chem. Soc.* 1985, **107,** 3902–3909
26 Molecular Simulations. *Quanta*. Molecular Simulations, Waltham, Massachusetts, 1993
27 Mulholland, A.J., and Richards, W.G. Calculations on the substrates of citrate synthase. I. Oxaloacetate. *J. Mol. Struct. (Theochem.)* 1998, **429,** 13–21
28 Wavefunction. *Spartan*, version 5.1. Wavefunction Inc., Irvine, California, 1995
29 Gaussian. *Gaussian*, revision A.6. Gaussian, Pittsburgh Pennsylvania, 1998
30 Fleming, I. *Frontier Orbitals and Organic Chemical Reactions*. John Wiley & Sons, New York, 1976
31 Van Berkel, W.J.H., and Müller, F. The temperature and pH dependence of some properties of *p*-hydroxybenzoate hydroxylase from *Pseudomonas fluorescens*. *Eur. J. Biochem.* 1989, **179,** 307–314
32 Spector, T., and Massey, V. Studies on the effector specificity of *p*-hydroxybenzoate hydroxylase from *Pseudomonas fluorescens*. *J. Biol. Chem.* 1972, **247,** 4679
33 Vervoort, J., Ridder, L., Van Berkel, W.J.H., and Rietjens, I.M.C.M. Flavoprotein monooxygenases: Mechanistic overview. In: *Flavins and Flavoproteins*. (Stevenson, K.J., Massey, V., and Williams, C.H. Jr, eds.) University of Calgary Press, Calgary, Alberta, Canada, 1996
34 Cremer, D. General and theoretical aspects of the peroxide group. In: *The Chemistry of Functional Groups: Peroxides* (Patai, S., ed.). John Wiley & Sons, New York, 1983
35 Vervoort, J., and Rietjens, I.M.C.M. Unifying concepts in flavin-dependent catalysis. *Biochem. Soc. Trans.* 1996, **24,** 127–130

Lars Ridder, Adrian J. Mulholland, Ivonne M.C.M. Rietjens, and Jacques Vervoort

Combined quantum mechanical and molecular mechanical reaction pathway calculation for aromatic hydroxylation by *p*-hydroxybenzoate-3-hydroxylase

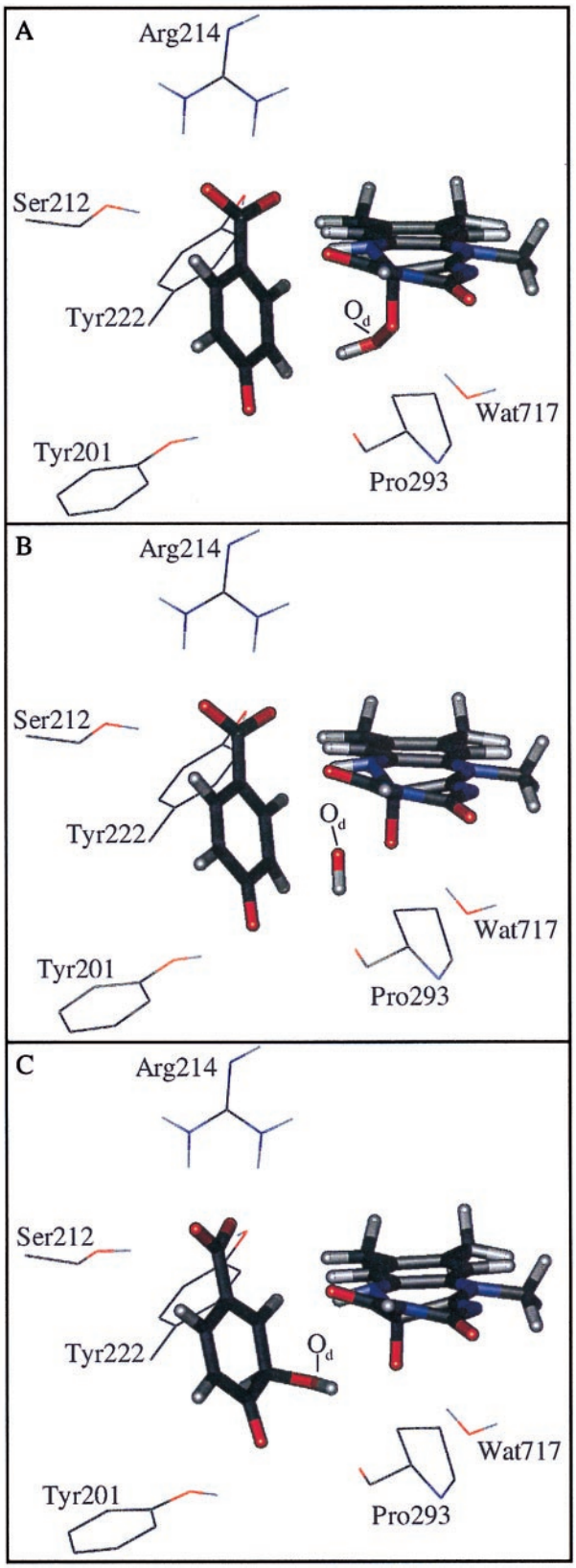

Color Plate 1 (left). The active site region in (a) the substrate–C4a-hydroperoxyflavin reactant state, (b) the transition state, and (c) the cyclohexadienone–C4a-hydroxyflavin product state. The MM atoms are shown as thin lines and the QM atoms are shown as thicker bonds.

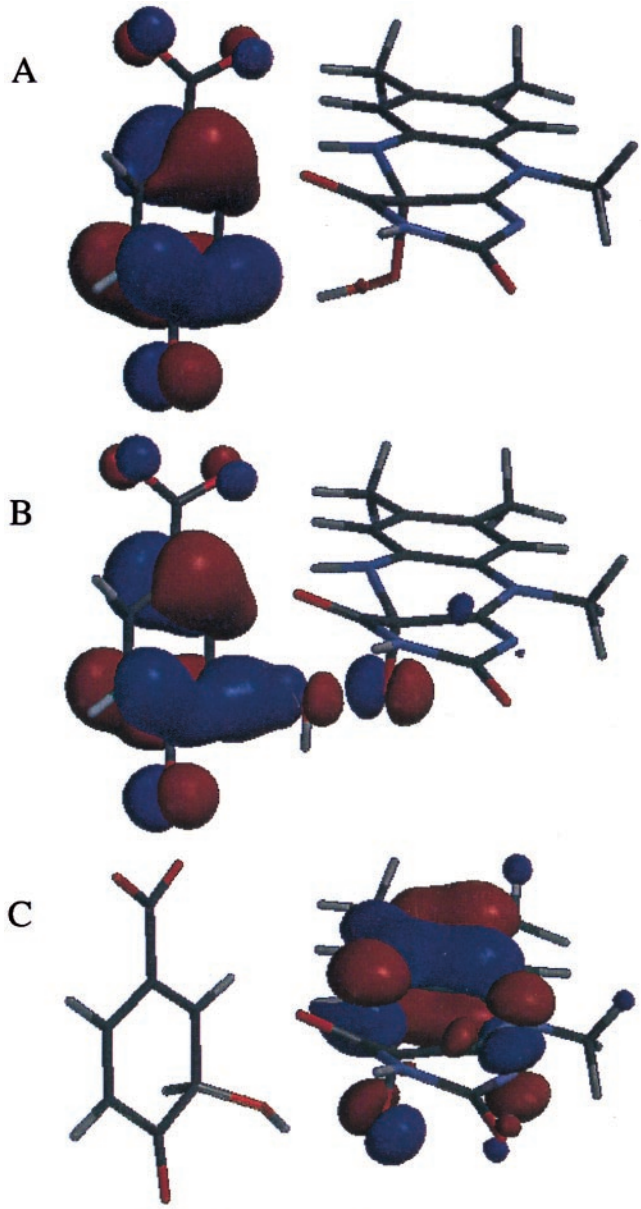

Color Plate 2 (above). Isodensity surface (0.03 electron/au^3) of the highest occupied molecular orbital in (a) the reactant state, (b) the transition state, and (c) the product state obtained by *in vacuo* single point calculations (AM1) of the geometries of the QM atoms obtained in the QM/MM reaction pathway calculation with dianionic 4-hydroxybenzoate.